The EMBO Journal Vol.18 No.9 pp.2323–2329, 1999

Two pacemaker channels from human heart with profoundly different activation kinetics

Andreas Ludwig, Xiangang Zong, Juliane Stieber, Roger Hullin[1], Franz Hofmann and Martin Biel[2]

Institut für Pharmakologie und Toxikologie der Technischen Universität München, Biedersteiner Straße 29, 80802 München and [1]Innere Medizin I, Universitätsklinik Großhadern, Marchioninistrasse 15, 81377 München, Germany

[2]Corresponding author
e-mail: biel@ipt.med.tu-muenchen.de

A.Ludwig and X.Zong contributed equally to this work

Cardiac pacemaking is produced by the slow diastolic depolarization phase of the action potential. The hyperpolarization-activated cation current (I_f) forms an important part of the pacemaker depolarization and consists of two kinetic components (fast and slow). Recently, three full-length cDNAs encoding hyperpolarization-activated and cyclic nucleotide-gated cation channels (HCN1–3) have been cloned from mouse brain. To elucidate the molecular identity of cardiac pacemaker channels, we screened a human heart cDNA library using a highly conserved neuronal HCN channel segment and identified two cDNAs encoding HCN channels. The *hHCN2* cDNA codes for a protein of 889 amino acids. The *HCN2* gene is localized on human chromosome 19p13.3 and contains eight exons spanning ~27 kb. The second cDNA, designated *hHCN4*, codes for a protein of 1203 amino acids. Northern blot and PCR analyses showed that both hHCN2 and hHCN4 are expressed in heart ventricle and atrium. When expressed in HEK 293 cells, either cDNA gives rise to hyperpolarization-activated cation currents with the hallmark features of native I_f. hHCN2 and hHCN4 currents differ profoundly from each other in their activation kinetics, being fast and slow, respectively. We thus conclude that hHCN2 and hHCN4 may underlie the fast and slow component of cardiac I_f, respectively.

Keywords: chromosome 19/HCN channel/heart/hyperpolarization/pacemaker current

Introduction

Cardiac pacemaking determines heart rate and rhythm and is generated by the slow membrane-depolarization phase occurring between action potentials (DiFrancesco, 1993; Irisawa *et al*., 1993). An important part of the ionic conductance underlying cardiac pacemaker depolarization was identified in the late 1970s and early 1980s (Brown *et al*., 1977; Yanagihara and Irisawa, 1980; DiFrancesco, 1981) and termed I_f (f for funny) or synonymously I_h (h for hyperpolarization activated). I_f is activated by membrane hyperpolarization and is carried by both Na^+ and K^+. Elevation of intracellular cAMP levels shifts the voltage dependence of I_f in the positive direction resulting in increased inward current at a fixed negative membrane potential. This is an important mechanism responsible for the acceleration of the heart rate in response to sympathetic stimulation (Brown *et al*., 1979). Muscarinic stimulation slows the heart rate, in part due to a decrease in cAMP level and a resulting reduction of the I_f current (DiFrancesco and Mangoni, 1994; Wickman *et al*., 1998). cAMP regulates the current by direct binding to the channel (DiFrancesco and Tortora, 1991). An I_f current has also been detected in a variety of neuronal cells (Pape, 1996; Luthi and McCormick, 1998). In the brain, a major function of the current is to control the rate of rhythmic oscillations of single neurons and neuronal networks (neuronal pacemaking).

Recently, three full-length cDNAs encoding hyperpolarization-activated cation channels (*HAC1*, *HAC2* and *HAC3*; Ludwig *et al*., 1998; corresponding to *mBCNG-2*, *mBCNG-1* and *mBCNG-4*; Santoro *et al*., 1998) have been cloned from mouse brain. In addition, a partial sequence representing a putative fourth member of the gene family was identified from mouse brain (*mBCNG-3*; Santoro *et al*., 1998). To avoid misunderstandings due to different naming of the same proteins, in this report we will use the recently proposed consensus nomenclature for cloned I_f channels (Clapham, 1998; Biel *et al*., 1999a). According to this nomenclature, I_f channels are designated as hyperpolarization-activated cyclic nucleotide-gated (HCN) channels. The family members are named as follows: *HCN1* corresponds to *HAC2* (*mBCNG-1*), *HCN2* corresponds to *HAC1* (*mBCNG-2*), *HCN3* corresponds to *HAC3* (*mBCNG-4*).

The primary sequences of HCN1–3 have an overall identity of ~60%, indicating that all three channels derive from a common evolutionary ancestor. HCN channels belong to the superfamily of voltage-gated cation channels characterized by the presence of six transmembrane helices (S1–S6) and an ion-conducting P region between the fifth and sixth segment. In addition, HCN channels, like the cyclic nucleotide-gated (CNG) channels, contain a cyclic nucleotide-binding domain (CNBD) in the C-terminus conferring channel modulation by direct interaction with cAMP or cGMP (for recent reviews see Zagotta and Siegelbaum, 1996; Clapham, 1998; Biel *et al*., 1999a,b).

In contrast to the central nervous system, there is only limited information available on the types of HCN channels underlying cardiac I_f currents. Northern blot and *in situ* hybridization experiments indicated that a transcript corresponding to HCN2 is present in mouse heart (Ludwig *et al*., 1998). However, it is not known whether the cardiac HCN2 isoform is identical to its neural counterpart, or whether other types of HCN channels are expressed in

heart. In this paper, we report the cloning of two full-length cDNAs encoding HCN channels from human heart tissue. When expressed in human embryonic kidney (HEK) 293 cells both cDNAs are translated into functional hyperpolarization-activated cation channels with distinct properties.

Results

Cloning of two cardiac pacemaker channels

In an attempt to identify the molecular identity of the cardiac I_f channel, we screened a cDNA library prepared from the atrioventricular node region of human heart with a highly conserved portion of the mouse brain HCN1 channel encoding the transmembrane segments S1–S6 and the CNBD (Ludwig *et al*., 1998). The cDNA clones obtained fell into two classes defined as *hHCN2* and *hHCN4*. The open reading frames (ORFs) of the *hHCN2* and *hHCN4* cDNAs predict proteins of 889 and 1203 amino acids, respectively. Both proteins contain six putative transmembrane segments, a pore region and a CNBD (Figure 1A) characterizing them as members of the family of HCN channels. The overall sequence identity between hHCN2 and hHCN4 is ~70%. The homology is highest in the transmembrane region and the CNBD with a sequence identity of 90%. The sequences of the putative pore regions are identical between hHCN2 and hHCN4 except for one conservative substitution. In contrast, both channels diverge markedly from each other in their cytoplasmic N- and C-termini. Notably, the C-terminus of hHCN4 is ~250 amino acids longer than that of hHCN2. An interesting feature of the two cDNAs is the extraordinarily high GC content at the 5′ end of the translated sequence (87% for hHCN2 and 77% for hHCN4 over the first 500 nucleotides); this is reflected in the high occurrence of proline and glycine amino acid residues in either N-terminus.

Genomic structure of the human HCN2 gene

A search of the DDBJ/EMBL/GenBank database with the *hHCN2* sequence identified the cosmid clones F18382 and R33683, which contained most of the human *HCN2* gene. These cosmids, which have been localized to chromsome 19p13.3, belong to a contig constructed as part of an ongoing project to map and sequence the entire human chromosome 19 (Ashworth *et al*., 1995). However, the two cosmids did not cover the *hHCN2* gene completely. To close the gap between the cosmids we amplified the intervening genomic sequence by PCR. The amplicon had a length of 1.2 kb and contained exon 5 of hHCN2. An additional sequence gap roughly in the middle of cosmid F18382 was reported to be unsequencable, i.e. recalcitrant to many sequencing chemistries. We subcloned and analyzed the corresponding segment, it contained 57 bp colinear to nucleotides 99–155 of the *hHCN2* cDNA, demonstrating that the reported gap contains part of exon 1. The complete genomic structure of *hHCN2* comprises eight exons spanning ~27 kb (Figure 1B). The sizes of introns ranges from ~13 kb (intron 1) to ~370 bp (intron 6).

Tissue distribution of hHCN2 and hHCN4 mRNA

Northern blot analysis demonstrated that both *hHCN2* (Figure 2A) and *hHCN4* mRNA (Figure 2B) are expressed in human heart. hHCN2 was also abundant in brain, whereas only a weak signal on longer exposure times was detected for hHCN4 in this tissue. The length of the hHCN2 and hHCN4 transcripts are 3.4 and 7.5 kb, which is consistent with the length of the cloned cDNAs. The expression of the two HCN channels in human cardiac tissues was further examined by RT–PCR with two primer pairs amplifying specifically hHCN2 and hHCN4, respectively. RT–PCR conditions were chosen that should be able to differentiate semiquantitatively a difference in mRNA expression levels. To prove this and to compare the expression of the two HCN channels with that of a well-known cardiac ion channel, we used a primer pair specific for human GIRK4 under the same conditions. GIRK4 is a subunit of the cardiac acetylcholine-activated potassium channel (I_{KACh}) and was shown to be expressed predominantly in the heart atrium and only marginally in the ventricle (Krapivinsky *et al*., 1995). Both hHCN2- and hHCN4-specific products were easily amplified from ventricular and atrial mRNA. The GIRK4 product was also generated readily from atrial mRNA, but only in very low amounts from ventricular mRNA indicating the validity of the PCR assay. Taken together these results suggest that *hHCN2* and *hHCN4* mRNAs are widespread throughout the human heart ventricle and atrium.

Electrophysiological characterization of the expressed hHCN2 and hHCN4 channel

For a functional characterization of the two channels, HEK 293 cells were transfected with expression vectors carrying the full-length coding sequence of hHCN2 and hHCN4, respectively. In whole-cell voltage–clamp mode, hyperpolarizing voltage steps negative to –60 mV induced inward currents in hHCN2- (Figure 3A) and hHCN4- (Figure 3B) expressing cells. No hyperpolarization-activated current was observed in cells transfected with empty expression vector (not shown). The peak tail current amplitudes of hHCN2 and hHCN4 showed a sigmoidal dependence on the test voltage (Figure 3C). The membrane potential of half-maximal activation ($V_{1/2}$) obtained by fits to Boltzmann equations was –97 ± 1 mV (n = 11) for the hHCN2 and –109 ± 1 mV (n = 20) for the hHCN4 current. The slope of the voltage dependence was somewhat steeper in hHCN2 (–6.3 ± 0.5 mV, n = 11) than in hHCN4 (–11.0 ± 0.6 mV, n = 20). It should be noted that the hHCN4 current did not reach a true steady state even after 3 s pulses. For this reason the actual difference in $V_{1/2}$ and slope factor between hHCN2 and hHCN4 may be smaller than predicted from our fits. Both channels exhibited marked differences in their activation kinetics. The hHCN2 current (Figure 3A) activated much more quickly than the hHCN4 current (Figure 3B, note also the different time scale). The current traces of either channel type could be fitted with a single exponential function when the initial delay in current activation was excluded. Time constants for hHCN2 activation ranged from 196 ± 11 ms (n = 11) at –140 mV to 463 ± 45 ms (n = 11) at –110 mV. In contrast, hHCN4 activated with a distinctly slower time course with time constants ranging from 659 ± 49 ms (n = 16) at –140 mV to 23 ± 9 s at –110 mV (n = 16) (Figure 3D).

To determine the ion selectivity of hHCN2 and hHCN4, we measured the current/voltage (I/V) relationship of the

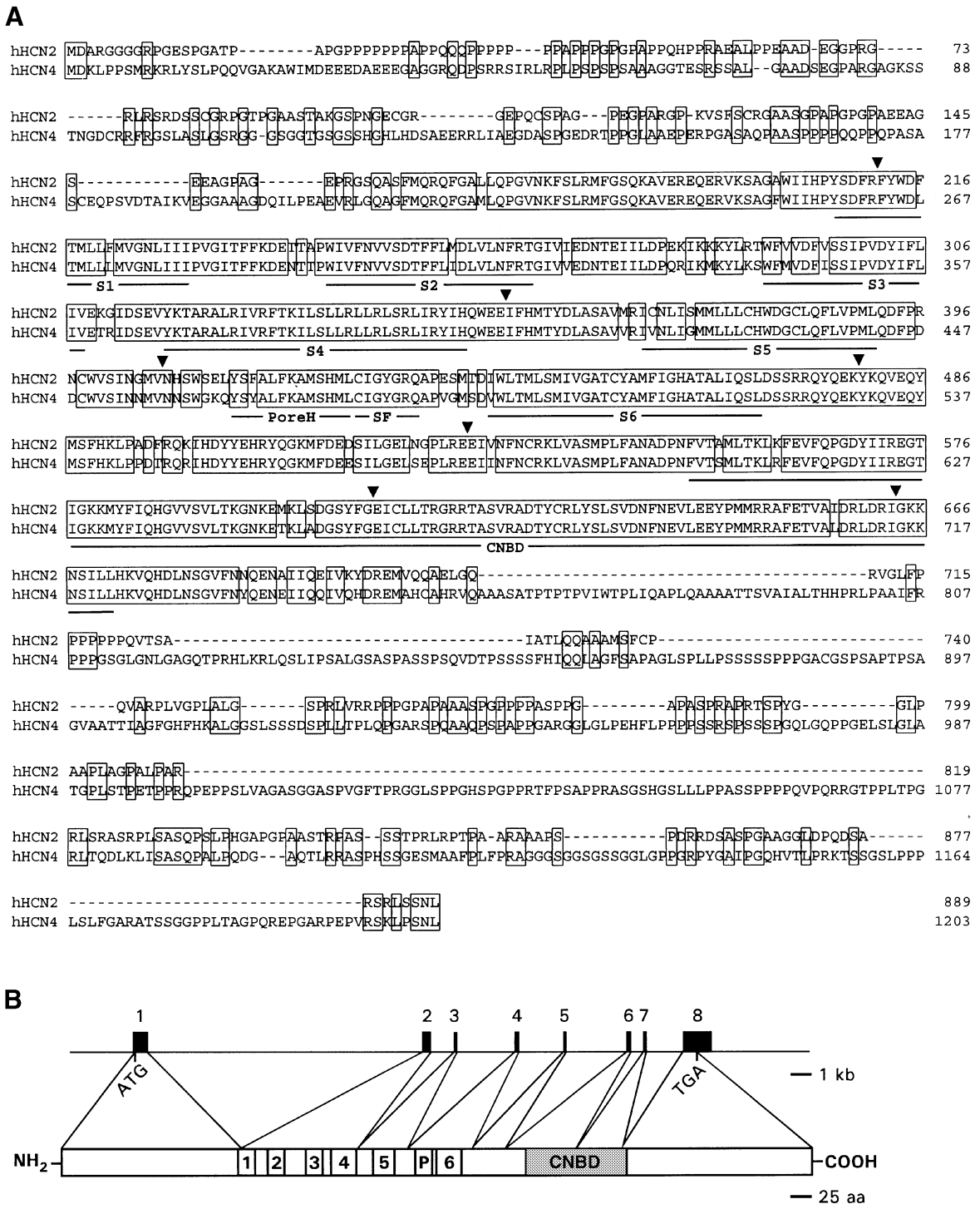

Fig. 1. Primary structure of the human HCN2 and HCN4 channels and organization of the *HCN2* gene. (**A**) Sequence alignment of hHCN2 and hHCN4. The six putative transmembrane segments (S1–S6), the pore region and the CNBD are underlined. The pore helix (PoreH) and the selectivity filter (SF) are delineated according to the *Streptomyces lividans* potassium channel crystal structure (Doyle *et al*., 1998). Exon–intron splicing sites of hHCN2 are marked by filled triangles. (**B**) Organization of the hHCN2 gene (upper) and corresponding distribution of exons in the domain structure of hHCN2 (lower). Upper: exons 1–8 are depicted by black boxes, the start and stop codons are indicated. Lower: transmembrane segments S1–S6 are numbered 1–6, P indicates the pore region.

fully activated channels (Figure 3E). The reversal potential at 30 mM extracellular K^+ was –23.8 ± 0.8 mV (n = 7) and –22.4 ± 2.2 mV (n = 6) for hHCN2 and hHCN4, respectively. The relative permeability ratio for Na^+ versus K^+ (P_{Na}/P_K), as determined by the Goldmann–Hodgkin–Katz equation, was 0.19 for hHCN2 and 0.22 for hHCN4, close to the value observed for native I_f.

A well-established feature of the native pacemaker current is the enhancement by cAMP resulting from a shift of the activation curve towards positive voltages. In accordance with these findings, in whole-cell mode measurements cAMP increased both the hHCN2 and the hHCN4 current by shifting the activation curves 15–16 mV in the positive direction (Figure 4A and B).

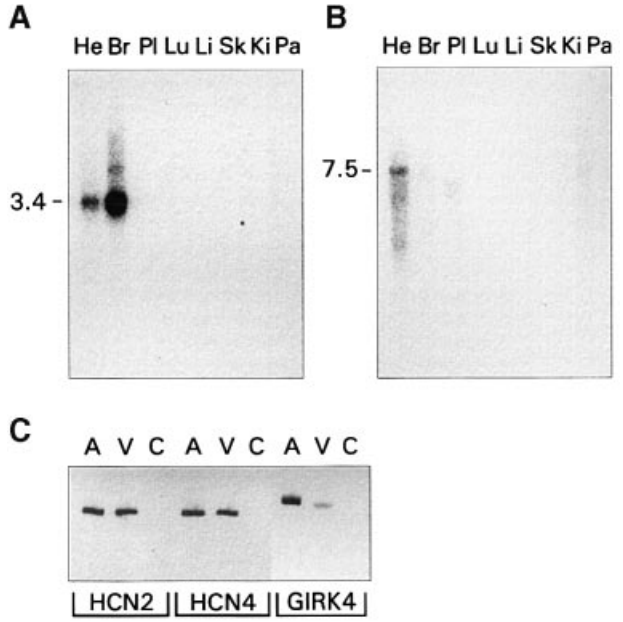

Fig. 2. Expression of HCN channel mRNAs. (A, B) Northern blot analysis of mRNA from human heart (He), brain (Br), placenta (Pl), lung (Lu), liver (Li), skeletal muscle (Sk), kidney (Ki) and pancreas (Pa). The blot was labeled with a probe specific for hHCN2 (**A**) and hHCN4 (**B**) and phosphorimaged for 16 h. The size of the transcripts is indicated in kilobases. (**C**) RT–PCR analysis. RT–PCRs with human heart ventricle (V), atrium (A) or without mRNA (C) as template was performed with primer pairs specific for hHCN2, hHCN4 or GIRK4. The sizes of amplicons were 230, 233 and 335 bp for HCN2, HCN4 and GIRK4, respectively.

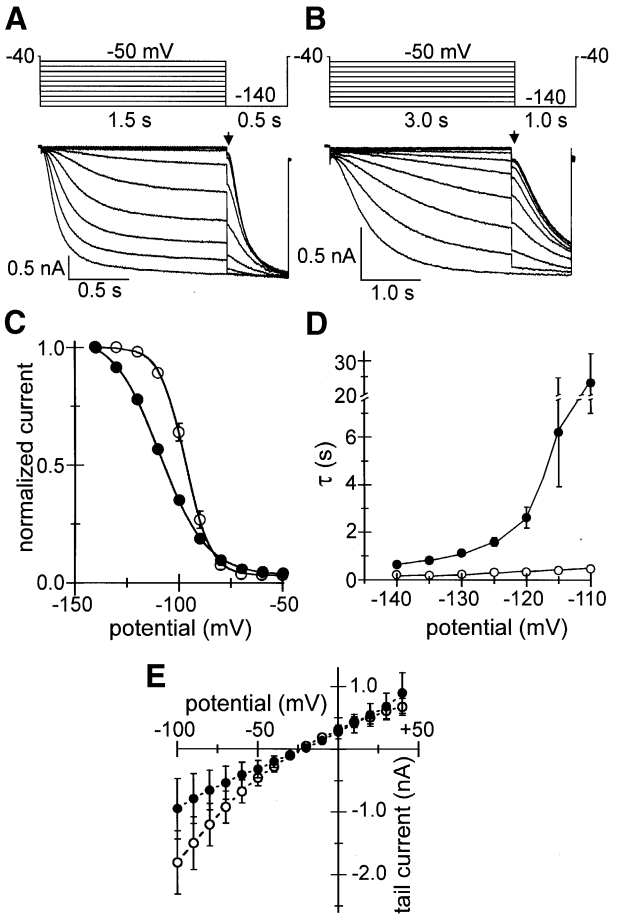

Fig. 3. Electrophysiological properties of the expressed hHCN2 and hHCN4 channel measured in whole-cell voltage clamp. (**A**) hHCN2 channel currents. Upper: voltage protocol. Cells were clamped from a holding potential of –40 mV to various voltages (–140 to –50 mV in 10 mV increments) for 1.5 s followed by a step to –140 mV. Lower: current traces of a cell expressing hHCN2. (**B**) hHCN4 channel currents. Upper: voltage protocol. As in (A) except for 3 s long prepulses. Lower: hHCN4 current traces. (**C**) Activation curves of hHCN2 (open circles) and hHCN4 (filled circles) currents. Tail currents measured immediately after the voltage step to –140 mV, arrow in (A) and (B), were normalized and plotted as a function of the preceding membrane potential. (**D**) Voltage dependence of activation kinetics. Current traces at voltages ranging from –140 to –110 mV from hHCN2- or hHCN4-expressing cells were fitted with a single exponential. The time constants for hHCN2 (open circles) and hHCN4 (filled circles) activation are plotted against the corresponding potentials. (**E**) Determination of the *I/V* relationship of the fully activated hHCN2 (open circle) and hHCN4 (filled circle) channel as described in the Materials and methods.

The $V_{1/2}$ values for the hHCN2 and the hHCN4 current were –97 ± 1 mV (n = 11) and –109 ± 1 mV (n = 20) in the absence, and –81 ± 2 mV (n = 11) and –94 ± 3 mV (n = 16) in the presence of 1 mM cAMP, respectively. Analogous to the native I_f current (DiFrancesco, 1991), cAMP also accelerated the activation kinetics of both channel types (Figure 4C and D). The hHCN2 current induced by a step to –140 mV was fitted by a single exponential with a time constant of 179 ms in the absence and 69 ms in the presence of 1 mM intracellular cAMP. Similarly, the hHCN4 activation kinetics at –140 mV accelerated with a time constant of 679 ms in the absence to 447 ms in the presence of 1 mM cAMP. Cyclic AMP did not increase further the amplitude of either the hHCN2 or the hHCN4 current when the channels were fully activated by hyperpolarization. For example, the maximal current at –140 mV for hHCN4 was 1.5 ± 0.3 nA (n = 16) in the absence of cAMP and 1.2 ± 0.2 nA (n = 10) after perfusion with 1 mM cAMP. These values are not statistically different (p >0.05).

Next, we determined the direct modulation of the two channels by cAMP using excised inside-out patches. In inside-out patches, $V_{1/2}$ was shifted by ~20–30 mV to more hyperpolarizing voltages with respect to the $V_{1/2}$ measured in whole-cell mode. A similar phenomenon has been observed for expressed HCN channels (Ludwig *et al.*, 1998) and also for the native I_f channel (DiFrancesco and Mangoni, 1994). Application of 10 μM cAMP to the intracellular side of the patch resulted in accelerated hHCN2 (Figure 4E) and hHCN4 (Figure 4F) channel opening at –120 and –150 mV. cAMP increased either current at –120 but not at –150 mV when the channels were already maximally activated by voltage. These results are in accordance with the effect of cAMP in whole-cell mode measurements (Figure 4A and B) showing a shift in the activation curve towards more positive voltages but no increase in the maximal current.

Finally, we determined the blocking efficiency of Cs^+ on the two pacemaker channels. The native I_f channel is blocked by low concentrations (0.1–5 mM) of extracellular Cs^+ (DiFrancesco, 1982; Denyer and Brown, 1990). Similarly, the expressed hHCN2 and hHCN4 channels activated by a step to –140 mV were blocked between 80 and 90% by 0.5 mM Cs^+ and ~95% by 2 mM Cs^+ (Figure 5A, B and E). In contrast, neither current was sensitive to 2 mM Ba^{2+} or 20 mM tetraethylammonium (TEA), two classic potassium channel blockers.

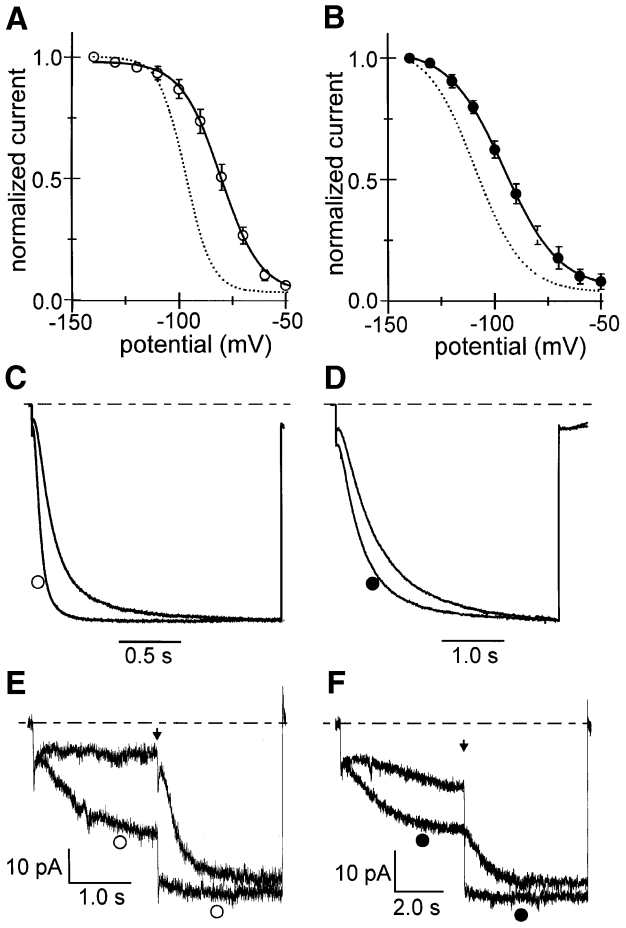

Fig. 4. Modulation of the hHCN2 and hHCN4 current by cAMP. (A, B) The voltage dependence of activation was determined from tail currents in whole-cell mode as described in legend to Figure 3C. (**A**) hHCN2 (open circles) and (**B**) hHCN4 currents (filled circles) were measured after intracellular perfusion for 1 min with 1 mM cAMP. For comparison the activation curves determined in the absence of cAMP (Figure 3C) are indicated by dotted lines. All curves represent fits of the tail currents by Boltzmann functions. (C, D) Acceleration of channel activation kinetics by cAMP. In whole-cell mode, the hHCN2 current (**C**) and the hHCN4 current (**D**) were fully activated by a step to –140 mV from a holding potential of –40 mV in the absence of cAMP (no symbol) or after intracellular perfusion for 1 min with 1 mM intracellular cAMP (open and filled circle, respectively). Normalized current traces are shown averaged from 11 cells under each condition (C) and from 16 and 10 cells in the absence respective presence of cAMP (D). (E, F) Direct modulation of hHCN2 (**E**) and hHCN4 (**F**) channels by cAMP measured in inside-out patches. Currents were evoked by clamping from a holding potential of –40 to –120 mV followed by a step (indicated by an arrow) to –150 mV. Traces were obtained in the absence (no symbol) and the presence of 10 μM cAMP in the bath solution [open circle (E), filled circle (F)].

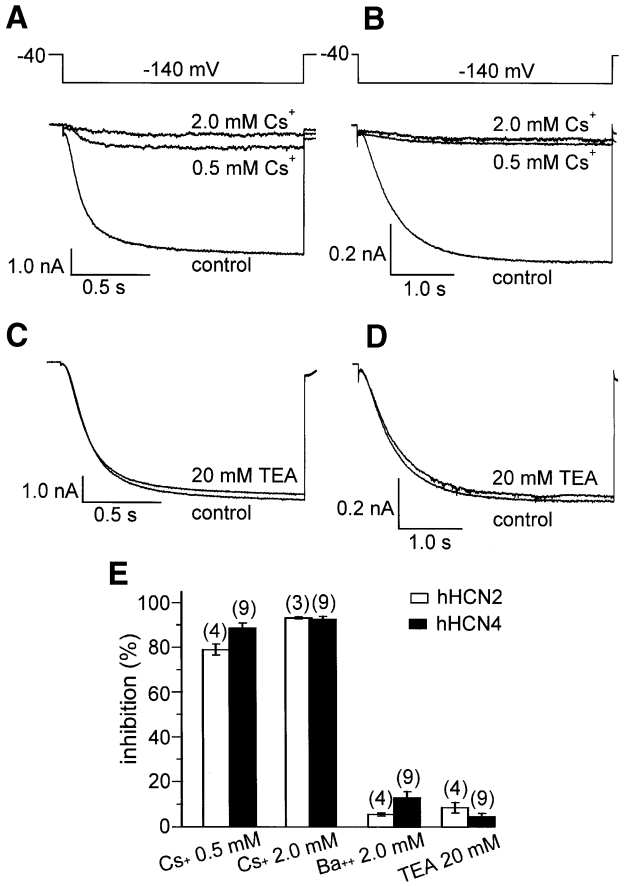

Fig. 5. (A, B) Effect of extracellular Cs^+, TEA and Ba^{2+} on the two HCN currents. HHCN2 (**A**) and hHCN4 (**B**) currents were evoked from a holding potential of –40 mV with a step to –140 mV for 3 and 4 s, respectively. Current traces in the absence and presence of 0.5 and 2.0 mM extracellular Cs^+ are shown. (C, D) Inhibition of whole-cell current by extracellular tetraethylammonium (TEA). hHCN2 (**C**) and hHCN4 (**D**) current traces in the absence and presence of 20 mM TEA are displayed. (**E**) Percentage inhibition of the current at –140 mV by 0.5 and 2 mM Cs^+, 2 mM Ba^{2+} and 20 mM TEA. Inhibition of the hHCN2 and hHCN4 currents is represented by open and filled bars, respectively, with the number of experiments shown in brackets above.

Discussion

The molecular nature of the channel(s) involved in the cardiac I_f current was not known until now. Here, we report the cloning of two pacemaker channels from human heart, hHCN2 and hHCN4 with different activation kinetics. The hHCN2 clone has an overall sequence identity of 94% with mHCN2 from mouse brain (Ludwig *et al*., 1998). No tissue-dependent alternative splicing events have been detected in the large number of hHCN2 clones examined indicating that identical HCN2 channels are present in heart and brain.

The hHCN4 channel probably represents the human full-length clone homologous to the partial cDNA sequence *mBCNG-3* (Santoro *et al*., 1998). This partial cDNA isolated from mouse brain codes for 500 amino acids of the core region of a HCN channel and its sequence is 98% identical to hHCN4.

The *hHCN2* and *hHCN4* cDNAs were cloned from a library prepared from human heart conduction tissue. The relative high expression of *hHCN2* and *hHCN4* mRNAs on Northern blots (Figure 2A and B) indicates that the two channels are expressed not only in the conduction tissues but also in contractile myocytes. This conclusion is consistent with the RT–PCR experiments demonstrating significant expression of both HCN mRNAs in cardiac ventricle and atrium. It is also compatible with previous results describing I_f currents in ventricular (Yu *et al*., 1995; Baker *et al*., 1997; Hoppe *et al*., 1998) and atrial (Thuringer *et al*., 1992; Porciatti *et al*., 1997) myocytes, as well as in the different conduction tissues (DiFrancesco, 1993). The ventricular myocyte I_f current has a $V_{1/2}$ between –95 and –135 mV, which is consistent with the $V_{1/2}$ values of the two HCN channels. In contrast, the I_f

current of sinoatrial node cells displays a varying but distinctly more positive $V_{1/2}$ ranging from –65 to –90 mV. The reason for the differing $V_{1/2}$ values between I_f from ventricular and sinoatrial node myocytes is unknown.

Both hHCN2 and hHCN4 exhibit properties corresponding to those of native I_f channels, i.e. activation at hyperpolarized membrane potentials, permeation of Na^+ and K^+, cAMP-dependent positive shift of the *I*/*V* relationship plus acceleration of channel activation and finally block by extracellular Cs^+. However, apart from these basic characteristics the two channels display profoundly different activation kinetics. The hHCN2 channel activates comparably quickly, whereas hHCN4 activation is markedly slower. Two kinetically distinct components of native I_f with time constants in the range of hundreds of milliseconds and seconds, respectively, have been described in neurons (Solomon and Nerbonne, 1993) and heart cells (DiFrancesco *et al*., 1986; Maruoka *et al*., 1994; Liu *et al*., 1996). This raises the possibility that native I_f may be generated by the concerted action of two distinct channels. Moreover, the zebrafish mutant *smo* (Baker *et al*., 1997) displays a reduced heart rate due to a diminished I_f current. Smo cardiomyocytes show a severe reduction in the fast kinetic component of I_f (time constant ~300 ms), whereas a slow component (time constant 2 s) remained unchanged. It was concluded that I_f is due to the activity of two channels and that the *smo* mutation selectively affects one of them. Taken together, the description of native I_f with two kinetic components and in particular the genetic evidence from the *smo* mutant strongly support the idea that two populations of channels with differing activation kinetics contribute to the I_f current. Hence, the results of this study suggest that HCN2 and HCN4 may underlie the fast respective slow component of I_f.

The structural basis for the differing activation kinetics of the two channels is not yet known. The core region including the transmembrane segments, pore and CNBD is 90% homologous between the two channel types. An intriguing possibility is that the long N- or C-terminus of hHCN4 interacts with the channel activation mechanism slowing it down. Further experiments will be necessary to test this hypothesis.

Native pacemaker channels probably form tetramers. The presence of both *hHCN2* and *hHCN4* mRNAs in cardiac tissues raises the possibility that the two channels may form heteromeric complexes *in vivo*. Although we can not rule out this possibility, our experimental findings do not support the existence of heteromeric channels. The expression of each subtype alone gave rise to functional channels indicating that the formation of hHCN2 and hHCN4 homomers is sufficient to make a pacemaker channel. Our preliminary analysis of currents induced by coexpression of hHCN2 and hHCN4 supports the notion that two distinct hHCN2 and hHCN4 channel populations are formed. In addition, the data from the *smo* mutant (Baker *et al*., 1997) favor the hypothesis that native pacemaker channels may be homomeric rather than heteromeric complexes.

Several inherited disorders of pacemaking, such as various forms of congenital sinus node dysfunction have been described (Saracheck and Leonard, 1972; Lehmann and Klein, 1978; Mackintosh and Chamberlain, 1979). The determination of the complete exon–intron organization of *hHCN2* should make it possible to screen genomic DNA samples of patients to detect possible links between these diseases and mutations of the *hHCN2* gene. Naturally, the gene encoding hHCN4 will also be a candidate in the search for genes underlying defects of cardiac pacemaking. Gene targeting may help to elucidate the precise role and relative importance of the two HCN channels for normal pacemaking activity.

Materials and methods

Molecular cloning of hHCN2 and hHCN4

A cDNA library was prepared from the atrioventricular node region of a human heart using pcDNAII vector (Invitrogen). Colonies (1×10^6) were screened with a ^{32}P-labeled probe corresponding to amino acids 96–566 of mHCN1 from mouse brain (Ludwig *et al*., 1998). Twenty-one independent clones were recovered and analyzed by restriction mapping and partial sequencing. Sixteen clones were classified as hHCN2, three of them contained the complete ORF. The length of the *hHCN2* cDNA sequence was 3406 bp. Five clones fell into a separate class designated hHCN4, two of them contained the full-length coding sequence. The 3′-untranslated region (UTR) of *HCN4* comprised ~2.6 kb and was characterized by restriction mapping and partial sequencing. The total length of the *hHCN4* cDNA was 6.8 kb. Two clones containing the entire ORF from each class were sequenced on both strands. Sequencing was carried out using a combination of manual sequencing with Sequenase v. 2.0 (Amersham) and automated sequencing on an ABI Prism 310 with BigDye terminator chemistry (Perkin Elmer) and a LI-COR 4200 system (Li-Cor Biotechnology).

Genomic structure of hHCN2

The exon–intron organization of the human *HCN2* gene was determined by comparing the *hHCN2* cDNA with the sequence of cosmid clones F18382 (accession No. AC005559 for the telomeric and AC005577 for the centromeric part) and R33683 (accession No. AC004449) from the DDBJ/EMBL/GenBank database. The segment between cosmids F18382 and R33683 was PCR amplified with the primers HAC1F9 (5′-CGGCGC-CAGTACCAGGAGAAGGT-3′) and HAC1R4 (5′-TCAGCATGGC-CGTGACGAAGTTGG-3′). Cosmid R31514, which overlaps the above cosmid clones (http://www-bio.llnl.gov/bbrp/genome/genome.html) was used as template. The gap in the reported sequence of cosmid F18382 between the telomeric and centromeric part was filled by subcloning and sequencing the *Nco*I (nucleotide 17768 of AC005559)–*Not*I (nucleotide 144 of AC005577) fragment of cosmid F18382. Cosmids F18382 and R31514 were kindly provided by the Human Genome Center at the Lawrence Livermore National Laboratory, CA.

RT–PCR and Northern blot analysis

Poly(A)$^+$ RNA from human heart left ventricle and right atrium was isolated and reverse transcribed using oligo(dT) primers. PCR amplification was performed for 30 cycles (annealing temperature 59°C) with 10 ng cDNA and the following primer pairs: 209F (5′-CGCCTGATCCGCTACATCCAT-3′) and 209R (5′-AGTGCGAAGG-AGTACAGTTCACT-3′) corresponding to amino acids 342–348 and 411–418 of hHCN2; 415F (5′-CCCGCCTCATTCGATATATTCAC-3′) and 415R (GAGCGCGTAGGAGTACTGCTTC-3′) corresponding to amino acids 393–399 and 463–469 of hHCN4; GIRK4F (5′-CCCCTGA-ACCAGACAGACATCA-3′) and GIRK4R (5′-CAGCTGGGTGTGTT-GGTCTCAT-3′) corresponding to amino acids 251–257 and 355–363 of GIRK4 (DDBJ/EMBL/GenBank accession No. X83582; Ashford *et al*., 1994). To exclude the amplification of potential contaminating genomic DNA primer pairs spanned at least one intron.

A Northern blot containing 2 μg poly(A)$^+$ RNA from multiple human tissues (Clontech) was sequentially hybridized with ^{32}P-labeled cDNA probes corresponding to nucleotides 765–1016 of hHCN2 and nucleotides 4513–4910 of hHCN4 and exposed to a BAS-MP image plate (Fuji) for 16 h.

Expression of HCN channels and electrophysiological recordings

The entire coding regions of *hHCN2* (nucleotides –9 to 2961) and *hHCN4* (nucleotides 565–4281) were inserted into the *Eco*RI–*Eco*RV and the *Eco*RI–*Xho*I sites respectively, of the pcDNA3 vector (Invitrogen) yielding the expression plasmids hHCN2/pcDNA3 and hHCN4/pcDNA3.

HEK 293 cells were transiently transfected using a calcium phosphate method as described by Biel *et al*. (1996). Currents were measured at room temperature 2–3 days after transfection using either the whole-cell or inside-out patch–clamp technique. The extracellular solution contained: 110 mM NaCl, 0.5 mM $MgCl_2$, 1.8 mM $CaCl_2$, 5 mM HEPES, 30 mM KCl, pH 7.4 (NaOH). The intracellular solution contained: 130 mM KCl, 10 mM NaCl, 0.5 mM $MgCl_2$, 1 mM EGTA, 5 mM HEPES, pH 7.4 (KOH). The *I*/*V* relation of the fully activated HCN channels (Figure 3E) was determined as follows: steps to test voltages (range –100 to +40 mV) were applied after a prepulse to –140 mV (1.5 s for hHCN2 or 3 s for hHCN4; protocol A) or after a prepulse to –20 mV (protocol B). Tail current amplitudes were measured immediately after the test pulse. The difference of tail currents between protocol A and protocol B was determined and plotted against the test potential. Data were acquired at 1 kHz using a List EPC7 amplifier and pCLAMP software (Axon instruments). Average values are given as mean ± SEM.

The DDBJ/EMBL/GenBank accession numbers for the reported sequences are AJ012582 for hHCN2, AJ132429 for hHCN4 and AJ133727–AJ133734 for exons and adjacent introns of hHCN2.

Acknowledgements

The atrioventricular node region of a heart of a patient undergoing transplantation was kindly provided by Drs J.Şchreieck and C.Schmitt, Klinikum rechts der Isar, Technische Universitat Munchen together with Dr M.Overbeck, Deutsches Herzzentrum Munchen. We thank Anna Klein, Richard Ohnhauser and Annemarie Vater for excellent technical assistance. This work was supported by grants from Deutsche Forschungsgemeinschaft and Fond der Chemischen Industrie.

References

Ashford,M.L.J., Bond,C.T., Blair,T.A. and Adelman,J.P. (1994) Cloning and functional expression of a rat heart K_{ATP} channel. *Nature*, **370**, 456–459.

Ashworth,L.K. *et al*. (1995) An integrated metric physical map of human chromosome, 19. *Nature Genet.*, **11**, 422–427.

Baker,K., Warren,K.S., Yellen,G. and Fishman,M.C. (1997) Defective 'pacemaker' current (I_h) in a zebrafish mutant with a slow heart rate. *Proc. Natl Acad. Sci. USA*, **94**, 4554–4559.

Biel,M., Zong,X., Ludwig,A., Sautter,A. and Hofmann F. (1996) Molecular cloning and expression of a modulatory subunit of the cyclic nucleotide-gated cation channel. *J. Biol. Chem.*, **271**, 6349–6355.

Biel,M., Ludwig,A., Zong,X. and Hofmann F. (1999a) Hyperpolarization-activated cation channels: a multi-gene family. *Rev. Physiol. Biochem. Pharmacol.*, **136**, 165–181.

Biel,M., Zong,X., Ludwig,A., Sautter,A. and Hofmann,F. (1999b) Structure and function of cyclic nucleotide-gated channels. *Rev. Physiol. Biochem. Pharmacol.*, **135**, 151–171.

Brown,H.F., Giles,W. and Noble,S.J. (1977) Membrane currents underlying activity in frog sinus venosus. *J. Physiol.*, **271**, 783–816.

Brown,H.F., DiFancesco,D. and Noble,S.J. (1979) How does adrenalin accelerate the heart? *Nature*, **280**, 235–236.

Clapham,D.E. (1998) Not so funny anymore: pacing channels are cloned. *Neuron*, **21**, 5–7.

Denyer,K.C. and Brown,H.F. (1990) Pacemaking in rabbit isolated sino-atrial node cells during Cs^+ block of the hyperpolarization-activated current, I_f. *J. Physiol.*, **429**, 401–409.

DiFrancesco,D. (1981) A new interpretation of the pacemaker current in calf Purkinje fibres. *J. Physiol.*, **314**, 359–376.

DiFranceso,D. (1982) Block and activation of the pacemaker channel in calf Purkinje fibres: effects of potassium, caesium and rubidium. *J. Physiol.*, **329**, 485–507.

DiFrancesco,D. (1993) Pacemaker mechanisms in cardiac tissue. *Annu. Rev. Physiol.*, **55**, 455–472.

DiFrancesco,D. and Tortora,P. (1991) Direct activation of cardiac pacemaker channels by intracellular AMP. *Nature*, **351**, 145–147.

DiFrancesco,D. and Mangoni,M. (1994) Modulation of single hyperpolarization-activated channels (I_f) by cAMP in the rabbit sino-atrial node. *J. Physiol.*, **474**, 473–482.

DiFrancesco,D., Ferroni,A., Mazzanti,M. and Tromba,C. (1986) Properties of the hyperpolarizing-activated current (I_f) in cells isolated from the rabbit sino-atrial node. *J. Physiol.*, **377**, 61–88.

Doyle,D.A., Cabral,J.M., Pfuetzner,R.A., Kuo,A., Gulbis,J.M., Cohen, S.L., Chait,B.T. and MacKinnon,R. (1998) The structure of the potassium channel: molecular basis of K^+ conduction and selectivity. *Science*, **280**, 69–77.

Hoppe,U.C., Jansen,E., Sudkamp,M. and Beuckelmann,D.J. (1998) Hyperpolarization-activated inward current in ventricular myocytes from normal and failing human hearts. *Circulation*, **97**, 55–65.

Irisawa,H., Brown,H.F. and Giles,W. (1993) Cardiac pacemaking in the sinoatrial node. *Physiol. Rev.*, **73**, 197–227.

Krapivinsky,G., Gordon,E.A. Wickman,K., Velimirovic,B., Krapivinsky,L. and Clapham,D.E. (1995) The G-protein-gated atrial K^+ channel I_{KACh} is a heteromultimer of two inwardly rectifying K^+-channel proteins. *Nature*, **374**, 135–141.

Lehmann,H. and Klein,U.E. (1978) Familial sinus node dysfunction with autosomal dominant inheritance. *Br. Heart J.*, **40**, 1314–1316.

Liu,Z.W., Zou,A.R., Demir,S.S., Clark,J.W. and Nathan,R.D. (1996) Characterization of a hyperpolarization-activated inward current in cultured pacemaker cells from the sinoatrial node. *J. Mol. Cell. Cardiol.*, **28**, 2523–2535.

Ludwig,A., Zong,X., Jeglitsch,M., Hofmann,F. and Biel,M. (1998) A family of hyperpolarization-activated mammalian cation channels. *Nature*, **393**, 587–591.

Luthi,A. and McCormick,D.A. (1998) H-current: properties of a neuronal and network pacemaker. *Neuron*, **21**, 9–12.

Mackintosh,A.F. and Chamberlain,D.A. (1979) Sinus node disease affecting both parents and both children. *Eur. J. Cardiol.*, **10**, 117–122.

Maruoka,F., Nakashima,Y., Takano,M., Ono,K. and Noma,A. (1994) Cation-dependent gating of the hyperpolarization-activated cation current in the rabbit sino-atrial node cells. *J. Physiol.*, **477**, 423–435.

Pape,H.C. (1996) Queer current and pacemaker: the hyperpolarization-activated cation current in neurons. *Annu. Rev. Physiol.*, **58**, 299–327.

Porciatti,F., Pelzmann,B., Cerbai,E., Schaffer,P., Pino,R., Bernhart,E., Koidl,B. and Mugelli,A. (1997) The pacemaker current I_f in single human atrial myocytes and the effect of β-adrenoceptor and A1-adenosine receptor stimulation. *Br. J. Pharmacol.*, **122**, 963–969.

Santoro,B., Liu,D.T., Yao,H., Bartsch,D., Kandel,E.R., Siegelbaum,S.A. and Tibbs,G.R. (1998) Identification of a gene encoding a hyperpolarization-activated pacemaker channel of brain. *Cell*, **93**, 717–729.

Sarachek,N.S. and Leonard,J.J. (1972) Familial heart block and sinus bradycardia: classification and natural history. *Am. J. Cardiol.*, **29**, 451–458.

Solomon,J.S. and Nerbonne, J.M. (1993) Two kinetically distinct components of hyperpolarization-activated current in rat superior colliculus-projecting neurons. *J. Physiol.*, **469**, 291–313.

Thuringer,D., Lauribe,P. and Escande,D. (1992) A hyperpolarization-activated inward current in human myocardial cells. *J. Mol. Cell. Cardiol.*, **24**, 451–455.

Wickman,K., Nemec,J., Gendler,S.J. and Clapham,D.E. (1998) Abnormal heart rate regulation in GIRK4 knockout mice. *Neuron*, **20**, 103–114.

Yanagihara,K. and Irisawa,H. (1980) Inward current activated during hyperpolarization in the rabbit sinoatrial node cell. *Pfluegers Arch.*, **388**, 11–19.

Yu,H., Chang,F. and Cohen,I.S. (1995) Pacemaker current I_f in adult canine cardiac ventricular myocytes. *J. Physiol.*, **485**, 469–483.

Zagotta,W.N. and Siegelbaum,S.A. (1996) Structure and function of cyclic nucleotide-gated channels. *Annu. Rev. Neurosci.*, **19**, 235–263.

Received February 1, 1999; revised and accepted March 4, 1999